JEM

Supplemental material

Ricard et al., https://doi.org/10.1084/jem.20182151

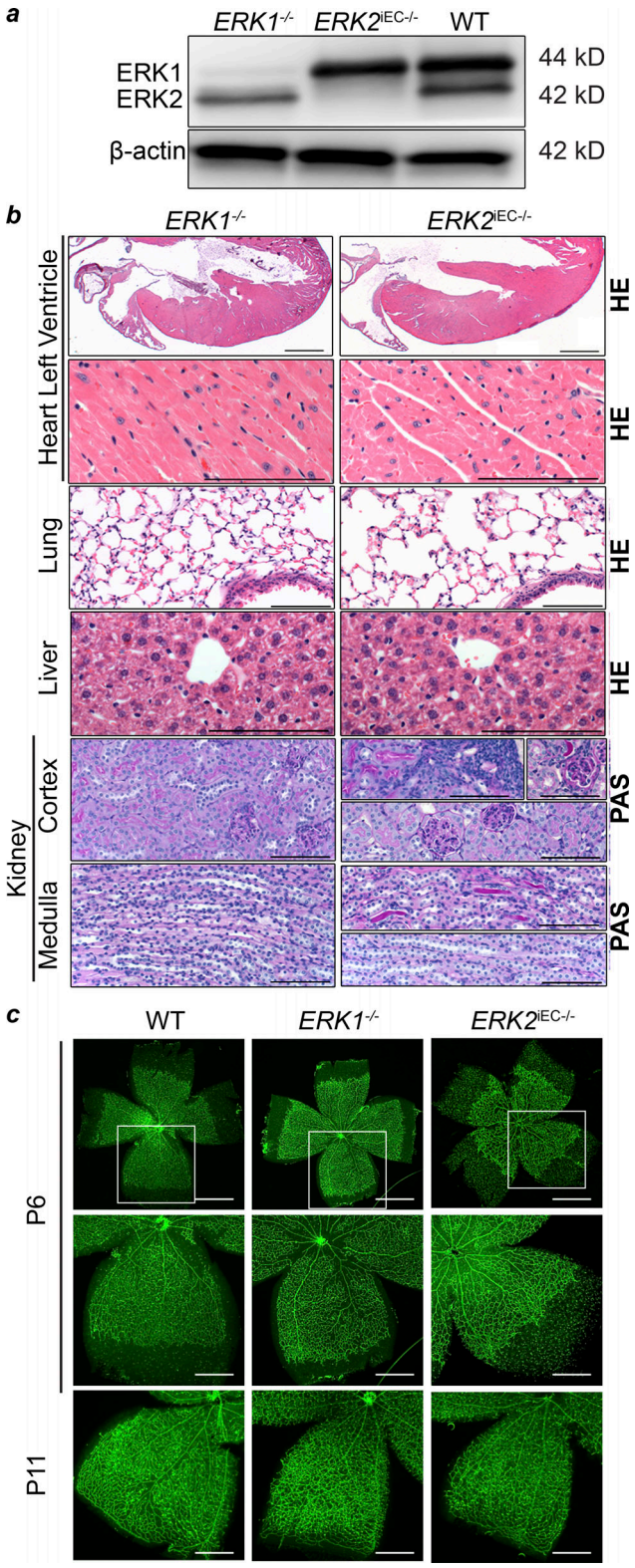

Figure S1. **Normal histology of heart, lung, liver, and kidney in *ERK1*$^{-/-}$ mice and *ERK2*$^{iEC-/-}$ mice. (a)** Western blot analysis of ERK1 and ERK2 expression in primary mouse pulmonary endothelial cells. Cells from *ERK2*$^{iEC-/-}$ mice were isolated 3 wk after tamoxifen injections. **(b)** Detailed review and comparison of representative sections of heart, lung, thymus, liver, and kidney from Erk1$^{-/-}$ (13 wk) and Erk2$^{iEC-/-}$ (21 and 33 wk) mice were as unremarkable and within normal limits for all tissues in all mice examined, except one Erk2$^{iEC-/-}$ mouse at week 21 that had renal pathological changes characterized as multifocal minimal chronic tubulointerstitial nephritis and infrequent glomerulosclerosis consistent with age (n = 2 mice per genotype). **(c)** Normal angiogenesis of the retina in *ERK1*$^{-/-}$ mice and delayed angiogenesis of the retina in *ERK2*$^{iEC-/-}$ mice. Tamoxifen was injected starting at day 1 after birth. Retinas were dissected at days 6 and 11 after birth (P6 and P11). Staining was done using isolectin B4. Scale bars represent 1 mm for top panels and 500 µm for middle and bottom panels.

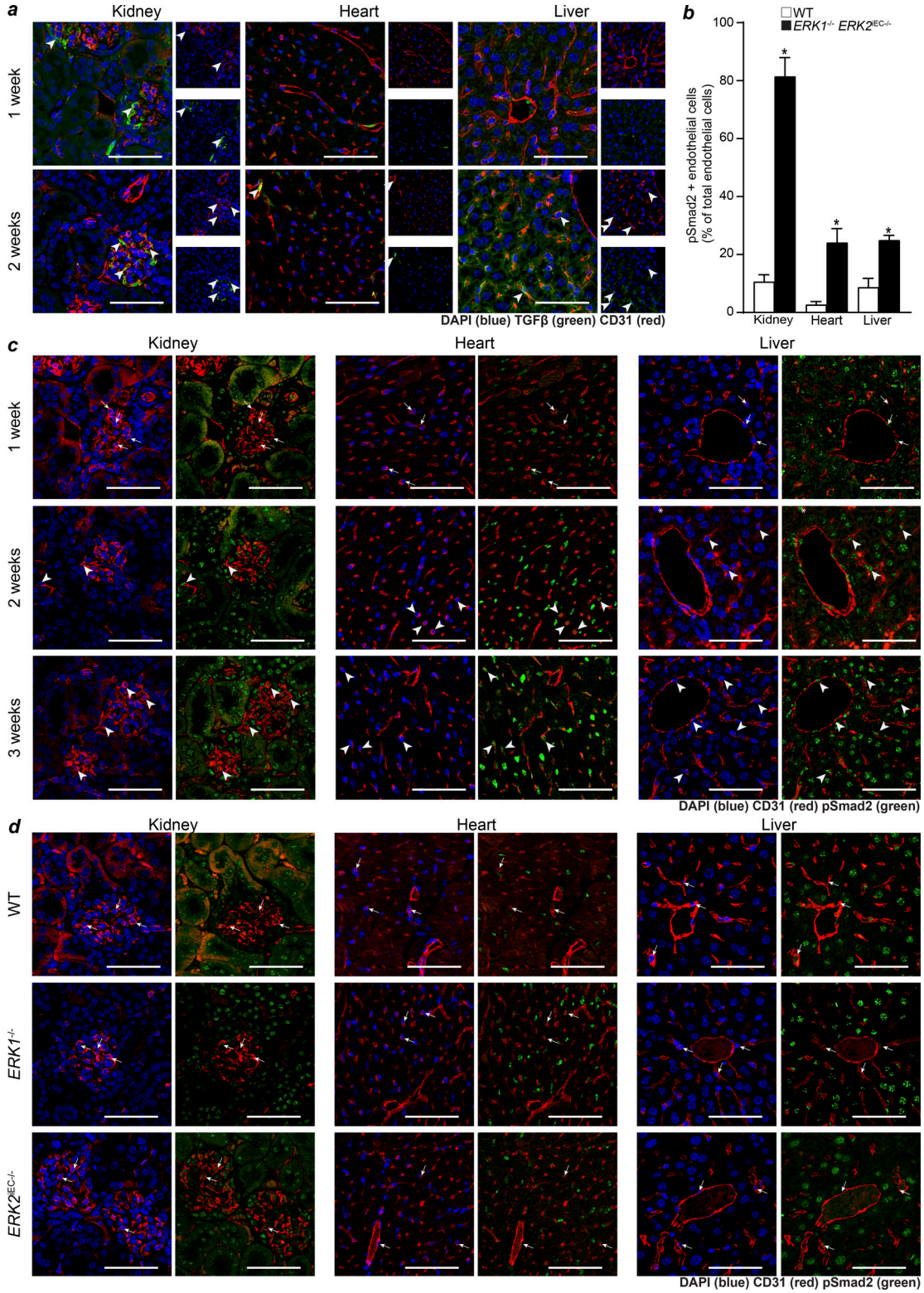

Figure S2. **TGFβ activation in endothelial cells from *Erk1*$^{-/-}$ *Erk2*$^{iEC-/-}$ mice. (a)** TGFβ staining in kidney, heart, and liver from *Erk1*$^{-/-}$ *Erk2*$^{iEC-/-}$ mice 1 and 2 wk after tamoxifen injections (representative of $n = 4$ mice per genotype). Scale bars, 50 µm. Arrowheads point to endothelial cells expressing TGFβ. The small picture represents the single channel of the large picture. **(b)** Quantification of the percentage of endothelial cells positive for pSmad2 staining 4 wk after tamoxifen injection ($n = 4$ mice per genotype). *, $P < 0.05$; Mann–Whitney *U* test. Error bars represent SEM. **(c)** pSmad2 staining in kidney, heart, and liver from *Erk1*$^{-/-}$ *Erk2*$^{iEC-/-}$ mice 1, 2, and 3 wk after tamoxifen injections (representative of $n = 4$ mice per genotype). Scale bars, 50 µm. Arrows point to endothelial cells with no or low pSmad2 staining. Arrowheads point to endothelial cells with intense pSmad2 staining. **(d)** pSmad2 in the endothelia of *Erk1*$^{-/-}$ mice and *Erk2*$^{iEC-/-}$ mice. pSmad2 staining in kidney, heart, and liver from *Erk1*$^{-/-}$ mice and *Erk2*$^{iEC-/-}$ mice (4 wk after tamoxifen [tam] injections; representative of $n = 4$ mice per genotype. Scale bars, 50 µm. Arrows point to endothelial cells with no or low pSmad2 staining.

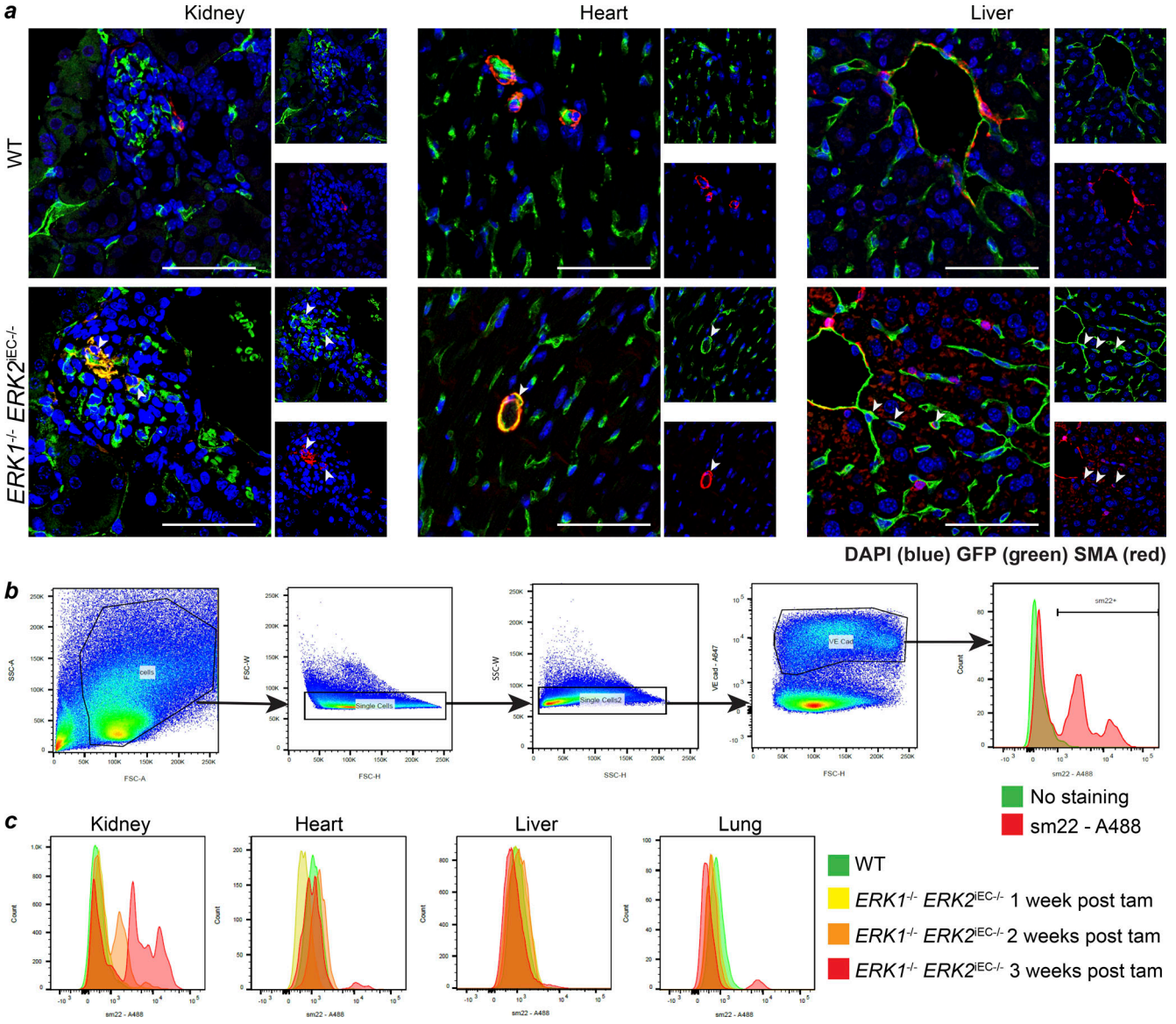

Figure S3. **Widespread EndMT in *Erk1*$^{-/-}$ *Erk2*$^{iEC-/-}$ mice. (a)** GFP and SMA staining in kidney, liver, and heart from Cdh5Cre-mTmG mice (denoted WT) and *Erk1*$^{-/-}$ *Erk2*$^{iEC-/-}$ mTmG mice 4 wk after tamoxifen injections (representative of n = 4 mice per genotype). Scale bars, 50 µm. Arrowheads point to endothelial cells expressing SMA. The small picture represents the single channel of the large picture. **(b and c)** FACS analysis on cell suspension from kidney, liver, heart, and lung from *Erk1*$^{-/-}$ *Erk2*$^{iEC-/-}$ mice. **(b)** FACS strategy used to quantify the proportion of endothelial cells (VE-cadherin$^+$) expressing sm22α. **(c)** sm22α fluorescence intensity of VE-cadherin$^+$ cells of kidney, liver, heart, and lung from *Erk1*$^{-/-}$ *Erk2*$^{iEC-/-}$ mice at 1, 2, and 3 wk after tamoxifen injection (representative from n = 4 mice per genotype and time point). FSC-W, forward scatter–width; FSC-H; forward scatter–height; FSC-A, forward scatter–area; SSC-A, side scatter–area; SSC-W, side scatter–width.

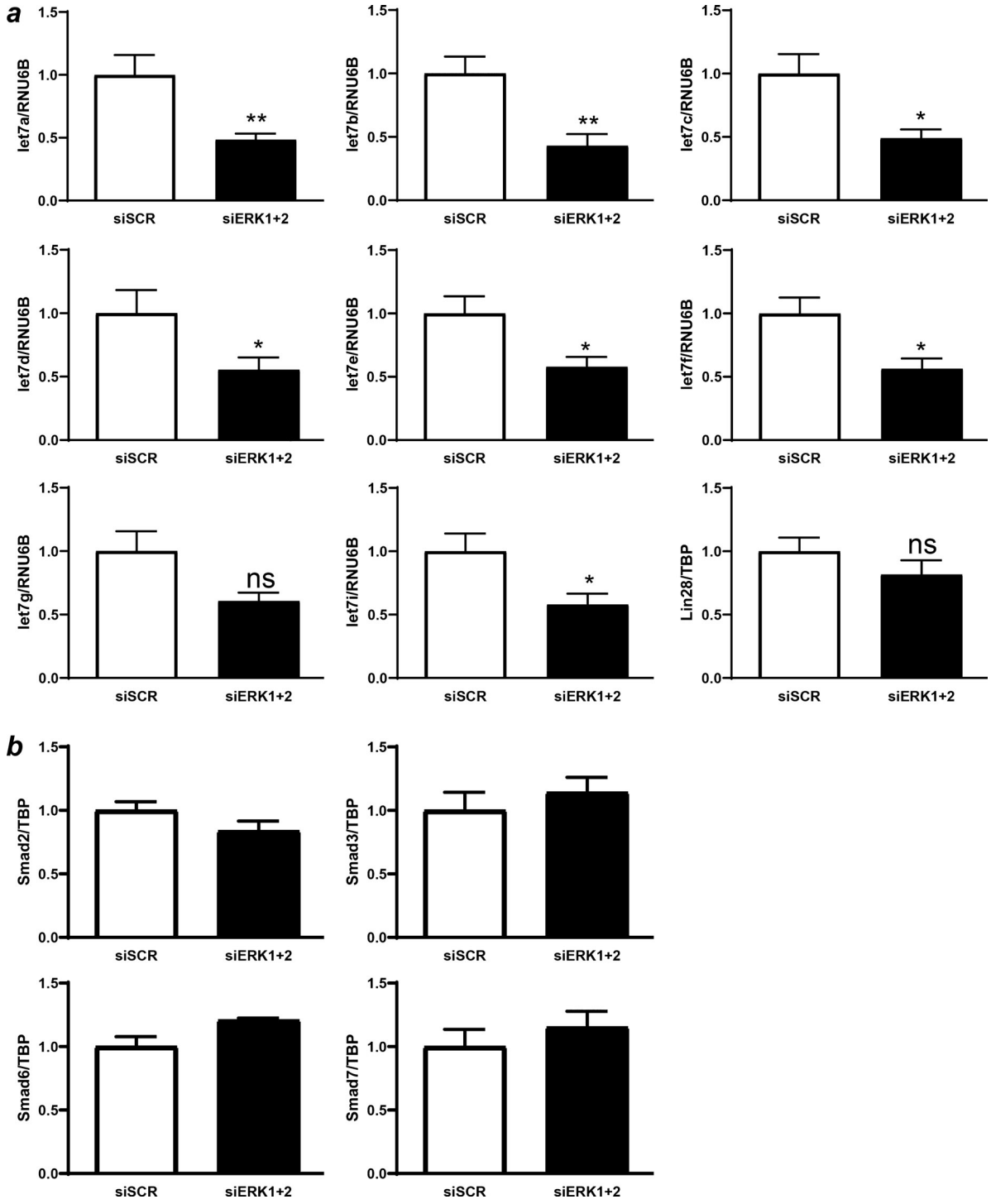

Figure S4. **Regulation of TGFβ pathway in ERK1/2 knockdown HUVECs. (a)** Expression level of let7 miRNA family members and Lin28 mRNA by qPCR on HUVECs treated by siERK1 and siERK2 for 4 d. (n = 8).**(b)** Smad2, smad3, smad6, and smad7 expression levels in HUVECs after siERK1 siERK2 treatment for 4 d. (n = 4). *, P < 0.05; **, P < 0.05; ns, not significant; Mann–Whitney U test. Error bars represent SEM.

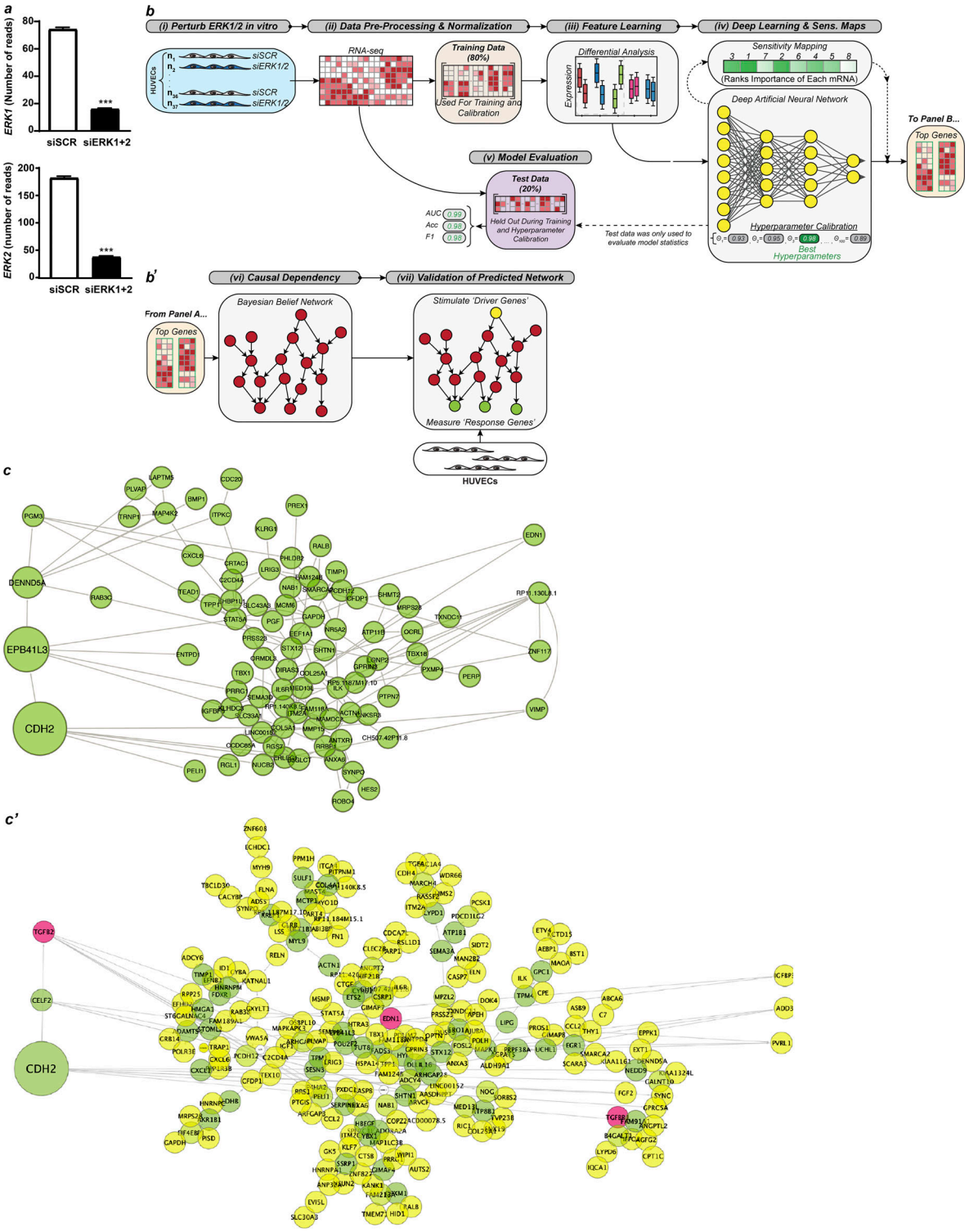

Figure S5. **Computational approach. (a)** ERK1 and ERK2 expression level determined by RNA-seq on HUVECs treated with siERK1 and siERK2 for 4 d (n = 18 for siSCR and n = 19 for siERK1 siERK2). ***, P < 0.001; Mann–Whitney U test. **(b and b')** Overall analysis strategy. (i) Perturbation of HUVECs with siSCR or siERK1/2. (ii) RNA-seq data were processed, normalized, and split into training and test data matrices as described in Materials and methods. (iii) Feature learning via differential expression (false-discovery corrected P < 1E-35), (iv) DANN (with inner cross-validation loop for tuning hyperparameters) trained to predict siSCR or siEKR1/2 classes, in combination with sensitivity mapping to determine the most informative genes. (v) Evaluating the trained DANN using the held-out test dataset. **(b)** Prediction of network structures and experimental validation. (vi) The most informative genes are used to build BBNs to determine causal drivers. (vii) Predicted BBNs are experimentally validated using in vitro cultured HUVECs. **(c and c')** Alternative BBNs. DAG derived from the intersection of the top 100 most informative genes (c) or the intersection of the top 600 most informative genes (c'). Genes on the left side of the DAG are the most likely upstream causal drivers, while the genes on the right are the most likely downstream targets (determined based on incoming and outgoing edges). AUC, area under the curve.

Tables S1–S3 are provided online as separate Excel files, and Table S4 is provided as a Text file. Table S1 shows systemic hypertension in *Erk1*$^{-/-}$ *Erk2*$^{iEC-/-}$ mice. Table S2 shows differential analysis of RNA-seq from siSCR- or siERK1/2-treated HUVECs. Table S3 lists DANN hyperparameter search ranges and other model parameters. Table S4 lists sensitivity mapping rankings of the 983 input genes to DANNs.